2. Development of a novel *in situ* testing device for a Focussed Ion Beam system and a Scanning Electron Microscope

In situ mechanical testing procedures for small scale samples in the μm range are rare. For many biological materials sizes in the μm range are typical, such as airflow sensors on crickets and individual components of the hairy attachment systems in insects and geckos (Kiel, 1998; Gorb, 2000). A variety of methods and devices exist for the mechanical testing and analysis of conventional bulk samples in the cm and mm range. Downscaling such standard mechanical testing methods (tensile tests, compression tests and bending tests) for specimens in the μm and sub-μm range provides a number of challenges. The major problem in building suitable mechanical testing devices is the lack of appropriate load cells. These load cells must have a high force resolution in the μN or even nN range. At the same time, they must provide a maximum force in the order of several mN. The second problem is the necessary resolution in strain or displacement. Already the handling of μm-sized samples is very difficult and their correct mounting is not trivial. Handling and clamping the samples into a holder can mechanically damage them: cracks can be introduced or, if the clamping is too weak, they can be pulled out of the sample holder on loading.

The aim of this thesis was to develop an *in situ* mechanical testing method, which overcomes these problems. In this chapter, sample preparation techniques, testing procedures and the measurement of the force, strain and cross-sectional area will be described in detail.

2.1 Literature review

This chapter is a review of the literature to date on typical mechanical testing methods that were performed *in situ* and which provide a force and displacement range and resolution for mechanical testing of samples in the μm-range. The reviewed tests are listed in Table 2.1 according to the type of device used and its typical force range. Tensile tests were performed using AFM-based systems (Yu *et al.*, 2000), nanoindentation systems, and a combination of AFM-and nanoindentation systems (Tan and Lim, 2004), a self-constructed testing apparatus (Huang and Spaepen, 2000) or micro-electro-mechanical systems (MEMS) (Haque and Saif, 2001). Beam (cantilever) bending (Florano *et al.*, 1999) and three point bending (Espinosa *et*

al., 2002) systems exist, too, as well as compression tests (Uchic *et al.*, 2004). The tests were carried out either using an optical microscope or *in situ* in an SEM or a TEM.

Table 2.1.: Literature overview of typical mechanical testing methods performed *in situ* and providing a force and displacement range and resolution for mechanical testing of samples in the µm-range.

Sample material	Method/ mode	Force resolution [µN]	Maximum force [µN]	Displacement resolution [µm]	Maximum displacement [µm]	Reference
Tension						
Carbon nanotubes	AFM	0.01	9000	1	100	Yu *et al.,* 2000
Polymer fibres	AFM-based nanoindenter	0.08	10000	0.0005	5	Tan and Lim, 2004
Collagen fibres	Tensile testing apparatus	0.5	12	0.24	10000	Miyazaki and Hayashi, 1999
Single crystal Si	Tensile testing apparatus	1500	2450000	0.028	28	Suwito *et al.,* 1999
Ag, Cu, Al, Ag/Cu multilayers	Tensile testing apparatus	0.1 MPa		0.002 %		Huang and Spaepen, 2000
Polysilicon, Ni, Ni-Fe	Pull tab specimens	10	1000000	0.01	150	Greek *et al.,* 1997
Polysilicon, amorphous diamond, Ni, Ni-Co, Ni-Fe	Pull tab specimens	0.01	180000	1	75	Buchheit *et al.* (2003)
Al	MEMS	1.368 0.003	382 250	0.090 0.058	10	Haque and Saif, 2001
Al	MEMS	5		0.1		Haque and Saif, 2002
Cantilever, three- and four point bending						
Bone	Beam bending	50	700		350	Liu *et al.,* 1999
Single crystal Si, Si-Al	Beam bending	10		0.0005		Florano *et al.,* 1999
Polysilicone	Three point bending	10		0.001		Ding *et al.,* 2001
Au	Three point bending	0.033	9000	1	100	Espinosa *et al.,* 2002
Carbon fibres	Three point bending	100	140000	0.5	200	Longtin *et al.,* 2004
Silicon nitride	Three point bending	0.25	20000	0.0003	6	Zhang *et al.,* 2000

Some of the *in situ* testing methods will be described in detail to give an overview of the different testing methods, load cells, strain measurement techniques and samples used. The methods are sorted according to the mode of testing (tension, bending, compression) and the testing device used.

Tensile tests using AFM-based systems, nanoindentation systems or a combination of both

With tensile tests the Young's modulus, tensile strength and strain to failure of a sample can be determined. Among the different mechanical testing modes, tensile tests tend to be easier to analyse than those in bending and compression, particularly, when composite materials are tested.

Yu *et al.* (2000) investigated the tensile strength of multiwalled Carbon Nanotubes (CNT) (length 1.80 - 10.99 µm, diameter 4 - 10 nm) using two AFM Cantilevers *in situ* in an SEM. Using carbon deposition, they attached each end of a single CNT to the opposite tips of AFM cantilever probes. From SEM micrographs both the applied force through the deformation of the flexible cantilever and the change in length of the CNT could be measured.

Tan and Lim (2004) performed tensile tests on micro- and nanoscale fibers using an AFM-based nanoindentation system. Poly (L-lactic-co-glycolic acid) fibers (~25 µm diameter, 3 mm length) were glued to both the nanoindenter tip and the base using a custom-made holder. The force transducer of the nanoindenter was used to measure the tensile force. The microfibre was stretched by moving the stepper motor of the AFM system. The elongation of the fibre was measured by subtracting the elongation of the transducer spring from the total elongation. The load and the displacement resolution were about 80 nN and 0.5 nm, respectively. The maximum force and displacement were 10 mN and 5 µm, respectively. The experiment was monitored using an optical microscope.

Self constructed and commercial tensile testing apparatus

Miyazaki and Hayashi (1999) investigated collagen fibres obtained from the patellar tendon of a rabbit. A glass capillary was attached, using a cyanoacrylate adhesive, to a load cell with a force resolution of 0.5 µN. A second glass capillary was affixed opposite the first with the load cell. Both were mounted on a micromanipulator. A load was applied by moving the two glass capillaries apart. The displacement was measured using a video dimension analyser via

the microscope and the CCD camera. The maximum stroke was 10 mm with a displacement resolution of 0.24 μm.

Huang and Spaepen (2000) performed tensile tests on free standing Cu, Ag and Al films and Ag/Cu multilayers. They used a micro-tensile tester onto which the sample was mounted with copper grips on two sliders. The force was applied by moving one of the sliders. The force was measured by a load cell attached to the other slider. The displacement was measured *in situ* by using a laser diffraction unit, which monitors the relative movement of two laser spots which were projected onto the sample. The tensile tester had a stress resolution of 0.1 MPa and a strain resolution of 0.002 %.

Tensile tests on pull tab shaped specimens

Greek *et al.* (1996) produced and tested polysilicon samples in tension which were fixed at one end and had a free standing ring pull tab at the opposite. An arm with a probe mounted on a piezoelectric actuator equipped with a strain gauge force sensor was moved into the ring of the pull tabs of the samples. By moving the probe apart, a load was applied to the sample. The whole setup was built inside an SEM, where the testing procedure was monitored. The displacement resolution was 0.01 μm, the maximum displacement was 150 μm, the maximum force was 1 N and the force resolution was 10 μN.

Beam bending

The advantage of beam bending experiments is that small scale samples can be tested with relative ease and that the mounting of the samples is often easier compared to the mounting for tensile testing. They can be glued with one end to the holder or a special holder can be used to clamp the sample. Cantilever, three- and four-point bending tests can all be found in the literature, where the load can be applied to the sample using standard AFM or nanoindentation systems, micromanipulators and specially designed stages for mechanical testing.

Force-displacement curves on cantilevers are frequently measured by two different techniques: one uses a nanoindenter, another an AFM. Florano *et al.* (1999) and Ding *et al.* (2001) used a nanoindenter system for both load and displacement-controlled measurements. The nanoindenter used by Florano *et al.* (1999) had a displacement resolution of 0.5 nm and a load resolution of 10 μN. The load resolution of the nanoindenter of Ding *et al.* (2001) was

the same, the displacement resolution was 1.0 nm. Alternatively, load and displacement can be applied by an AFM system (Serre *et al.,* 1998) and the tip deflection can be measured with nanometric accuracy by a photo detector.

Liu *et al.* (1999) investigated cylindrical (length: ~ 2mm, diameter: 160 μm) bone specimens in bending. The cantilever bending tests were performed using a micromechanical testing instrument, consisting of a low speed motor, a sensitive piezoelectric load cell (resolution: 50 μN, maximum load: 700 μN), a dual mode amplifier, an optical working stage and a computer. The whole test was monitored by a video camera fitted onto an optical microscope.

Micro-electro-mechanical systems (MEMS)

The use of MEMS is a relatively new technique for tensile tests at the sub-micrometer level. They consist usually of interconnected comb structures which can be driven by electrostatic forces.

Haque and Saif (2001) designed a MEMS electrostatic comb drive actuator which generates tensile forces. The actuator was equipped with a grip and has a self-calibration mechanism. The grip was fitted to the gripping end of the specimen, fabricated using a photolithographic and ion etching process. The lateral comb drive actuator with 3150 combs generated a maximum force of 382 μN with a resolution of 1.368 μN and a maximum displacement of 10 μm. The 280 comb actuators provided 3 nN in force resolution and a displacement resolution of 58 nm after 2 μm of axial displacement. After the alignment of the specimen and the actuator, the whole setup was used in an SEM.

Compression tests

Uchic *et al.* (2004) used a FIB system to machine cylindrical compression samples into the surface of a bulk crystal, leaving the samples on the crystal. The size of the samples ranged from 0.5 to 40 μm in diameter, with an aspect ratio of 2:1 to 4:1. The samples were uniaxially compressed using a conventional nanoindentation device with a flat-punch indentation tip. Ni and Ni-alloys were used as sample materials.

Summary of the literature

A number of *in situ* mechanical testing methods for samples in the micrometer and sub-micrometer range are described in the literature. None of the methods reviewed were adaptable for mechanical testing of biological samples in the µm regime. The reasons for this are the following: i) They either have the necessary spatial or the necessary force resolution, but rarely have both, ii) conventional Atomic Force Microscope (AFM) (Yu *et al.*, 2000) and nanoindentation-based systems (typical force range: 0.08 µN–10 mN) (Tan and Lim, 2004) have the required force resolution and maximum force, but they are ordinarily not suited for *in situ* testing, iii) MEMS usually allow only small displacements and operate only in one predefined plane and are thus not suited for different sized specimens (Haque and Saif, 2001), vi) conventional *in situ* test rigs (force resolution 50 µN) (Liu *et al.*, 1999) have insufficient force and displacement resolution for specimens in the µm regime, and v) some of the testing methods need specially designed samples (Buchheit *et al.*, 2003).

2.2 Development of a device for *in situ* mechanical testing

The force measuring device, developed in collaboration with Kleindiek Nanotechnik, consists of a micromanipulator MM3A, a system with two rotational and one longitudinal axis developed by Kleindiek GmbH (Kleindiek Nanotechnik). The manipulator is driven by stepper piezo motors, which can be moved in five different gears with different step-sizes. In the finest gear the micromanipulator can move 2048 steps in each direction from its zero position. The step size depends on the length of the longitudinal axis of the manipulator. In the smallest gear, the smallest step size of the rotational axes at a fully retracted longitudinal axis is 8 nm and the displacement at a fully extracted longitudinal axis is 15 nm. A piezoresistive AFM tip (Nascatec) was attached to the micromanipulator using a barrel shaped holder. The holder adds an additional axis of rotation. It is fixed during the tests by a screw. A picture of the testing device is shown in Figure 2.1.
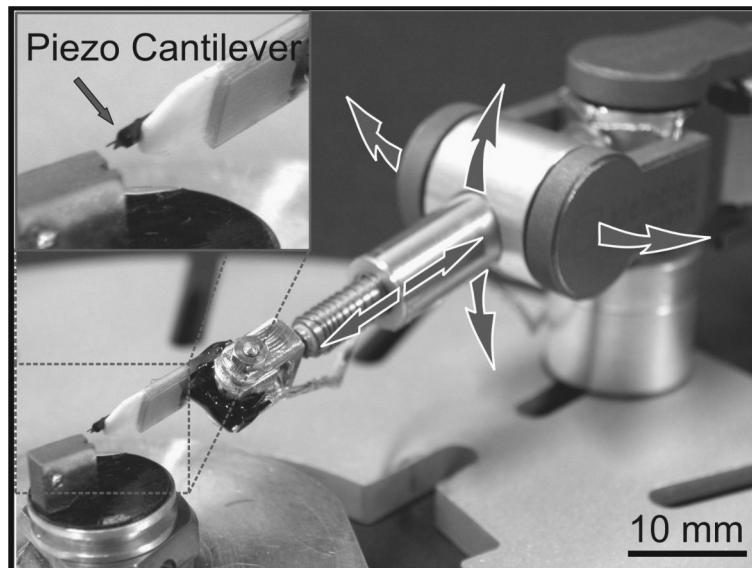
Figure 2.1: Force measuring device. A three-axis micromanipulator (Kleindiek Nanotechnik) equipped with an AFM tip (Nascatec) (Digital Camera).

Due to the small size and weight, the testing device is ideal for use in an SEM or FIB. Figure 2.2 shows a side view of the force measuring device, clamped onto the stage of an SEM (Leo 1530 VP).

Figure 2.2: Side view of the testing device clamped onto the stage of an SEM Leo 1530 VP (Digital Camera).

Piezoresistive AFM cantilevers are available with different stiffnesses ranging from 5 to 350 N/m. The AFM tips used in the experiments had a nominal stiffness of 270 N/m and could measure a maximum force of 1300 µN with a force resolution of 15 to 20 µN. The calibration of the AFM tips was performed before each test by moving the cantilever against a

micro-balance. The AFM tip consists of a piezocantilever with a Wheatstone bridge at its end. For small deformations the voltage changes linearly with an increase of the applied force.

2.3 Sample preparation

The FIB was found to be a powerful tool to explore the hierarchies of biological materials at the μm-scale, as demonstrated in Chapter 1.4, and was therefore used to prepare beam bending and tensile samples site specifically and precisely.

The sample preparation of beam bending samples and tensile testing samples used for this study will be demonstrated below on micromachined cantilevers of Kapton®, wood cell wall, a single seta of a beetle and sections of spider silk fibres.

2.3.1 Beam bending samples

Before sample preparation, all beam bending samples were coated with a thin carbon layer in order to minimise charging effects in the FIB or SEM.

Samples prepared from sheets

The polyimide Kapton® already exists in small sheets. It was hence straightforward to prepare microbeams from a small Kapton® sheet using the milling technique of the FIB system. This is demonstrated in Figure 2.3, which shows the contour of a cantilever, micromachined out of a 13.1 μm thick Kapton® sheet.
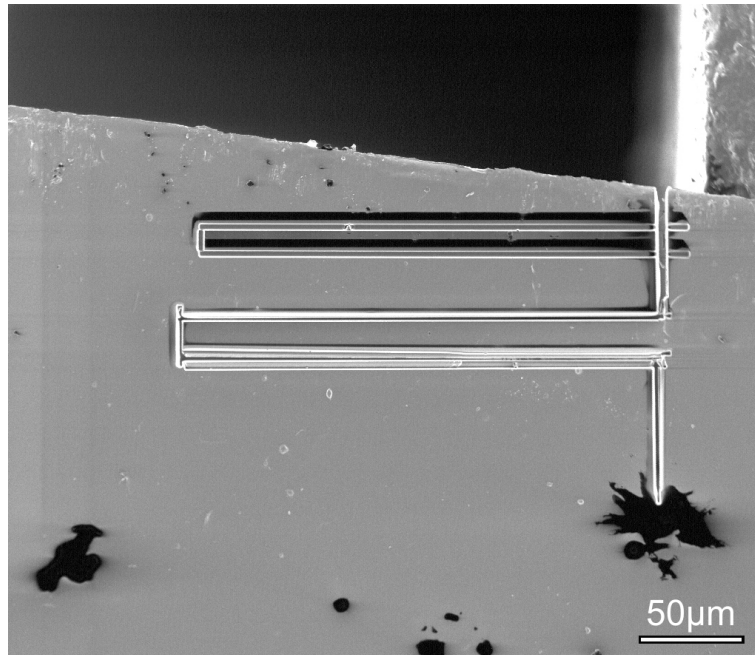
Figure 2.3: Micrograph of the contour of a micromachined polyimide Kapton® cantilever (SEM micrograph).

Samples prepared from structural materials

For the investigation of the material properties of a single wood cell wall, a cantilever was prepared from spruce wood. A small piece of spruce wood was cut with a razor blade. It was clamped into a custom made sample holder, which allows clamping sheet-like samples and the mounting of these in two different positions perpendicular to each other. In Figure 2.4 the ends of small rectangular wood cells, the so called tracheids, are visible. Using the FIB system, it was possible to cut free one of the cell walls (Figure 2.5).
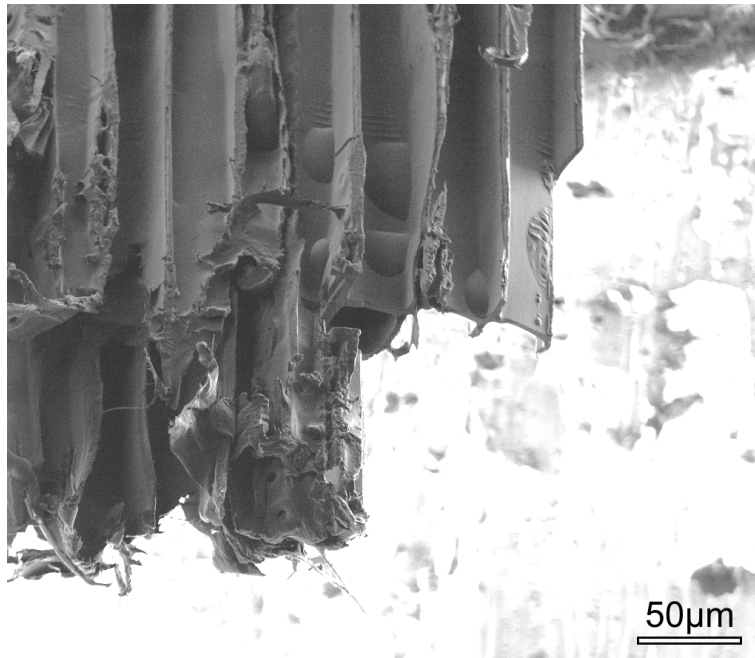
Figure 2.4: Small piece of spruce wood, cut with a razor blade (FIB micrograph).
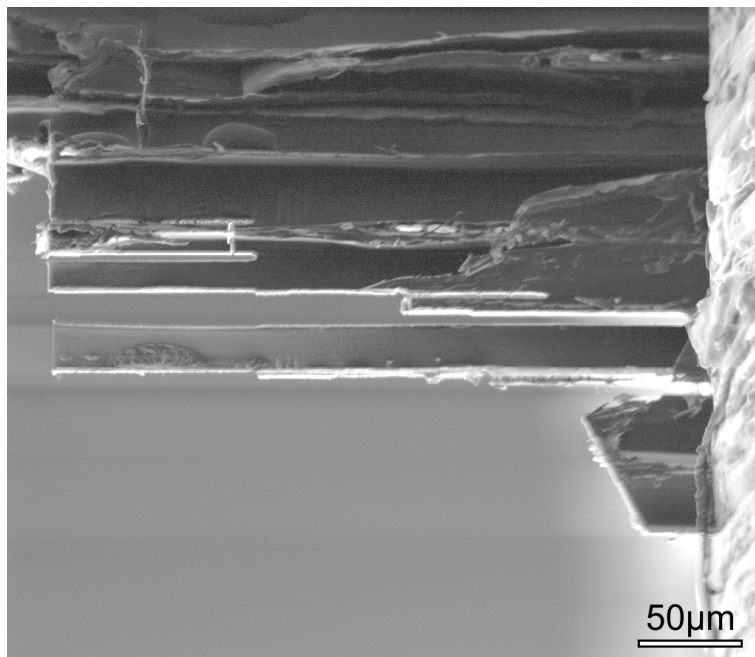
Figure 2.5: Cutting process during fabrication of a micro beam cut

out of a spruce wood tracheids (FIB micrograph).

The cutting of a cell wall cantilever allows measuring the mechanical properties of cell wall material of spruce wood.

2.3.2 Tensile test samples

Depending on the geometry of the initial sample, different techniques for sample preparation had to be used. The first method was used for short samples such as an individual seta of the hairy attachment system of the beetle *Gastrophysa viridula*. The second technique was used for long fibres or fibre-like specimens such as spider silk threads.

Compact tensile specimens

Samples of the setae of the beetle *Gastrophysa viridula*, which were about 30 to 40 µm in length and 1-2 µm in diameter, were prepared by mounting the terminal four segments of a leg of the beetle onto one edge of a small metal block, using silver paint. The AFM tip was then moved into contact with the setae of the beetle. Using tungsten deposition two setae were glued onto the AFM tip with tungsten tapes (beam current 150 pA; x, y, z: 7.0 µm × 2.5 µm × 1.0 µm, dwell time: 0.2 µs and overlap: -50 %). Thus affixed, the setae were cut at their base (beam current = 70 pA; Figure 2.6 a)). Then the micromanipulator was moved away from the beetle's leg and the metal block, onto which the leg had been glued, was rotated by 180° (Figure 2.6 b). Carefully moving the AFM tip with the setae in contact with the metal block, one was affixed to it with tungsten tapes (beam current = 150 pA; x, y, z: 7.0 µm × 2.5 µm × 1.0 µm; dwell time = 0.2 µs and overlap = -50 %) (Figures 2.6 c-d). Secured at both ends, the seta was ready for testing. Figures 2.6 a)-d) show the whole procedure of sample preparation.
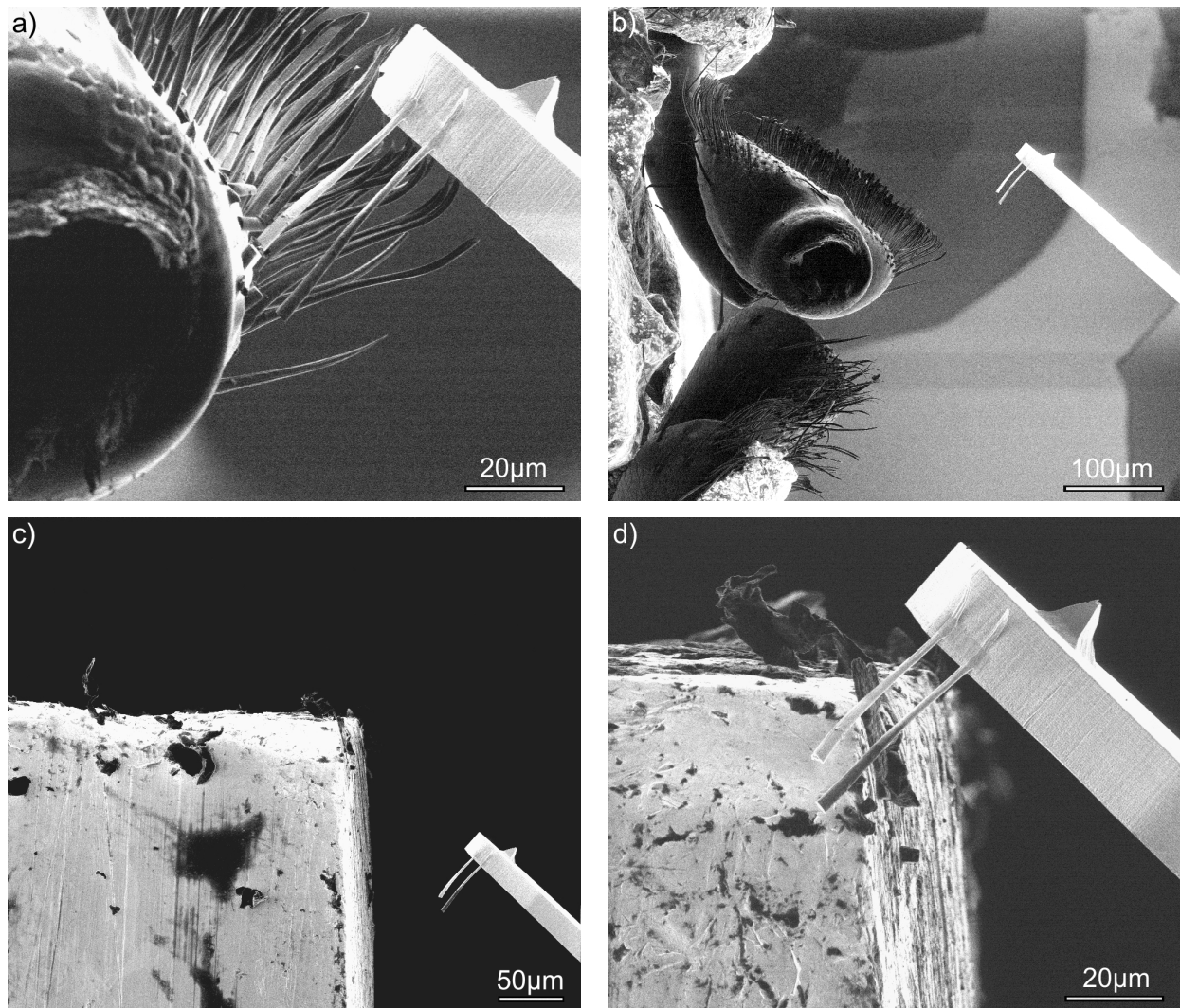
Figure 2.6: Sample preparation of single setae of the beetle *Gastrophysa viridula*:
a) two setae glued with tungsten tapes on the AFM tip, b) AFM tip moving away from the beetle's leg,
c) the metal block rotated by 180°, d) the setae in contact with the metal block (FIB micrographs).

Alternatively, seta samples were obtained by scratching the brush-like attachment pad with the AFM tip. In this way, some of the setae were broken off and stuck to the AFM tip because of electrostatic forces. These setae could also be affixed with one end to a metal block. After moving the AFM tip to a convenient position under the seta for optimum sample alignment, the seta was glued to the AFM tip using again tungsten deposition.

Long fibre-like tensile samples

A piece of spider silk was tightened between two metal blocks by gluing silk threads onto small pieces of carbon double sided adhesive pads, affixed to the top of the metal blocks. The metal blocks were mounted on a standard SEM/FIB sample holder. The sample holder was

afterwards transferred into the FIB. The AFM tip was brought into contact with the spider silk. Figure 2.7 shows the AFM tip positioned in contact under the spider silk fibre.
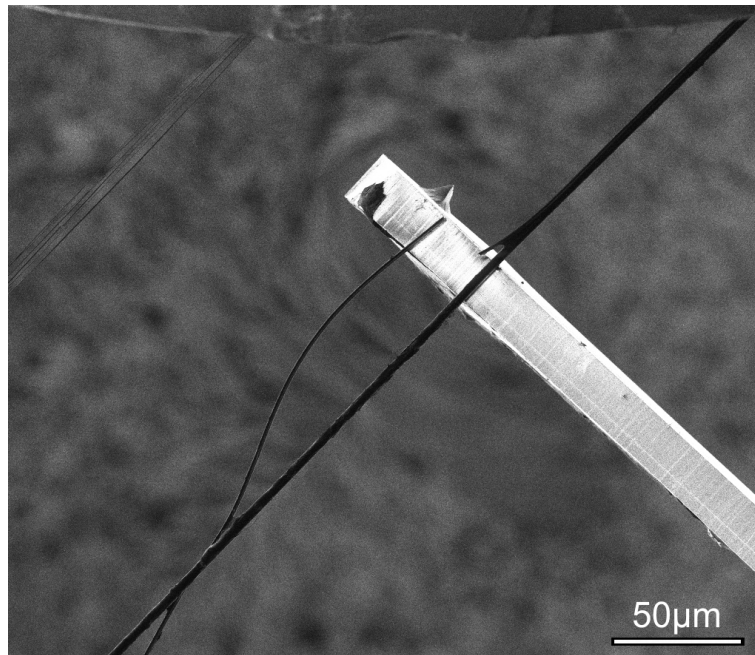

Figure 2.7: AFM tip in contact with the spider silk (FIB micrograph).

The silk was fixed to the AFM tip with small tungsten tapes (beam current = 150 pA; x, y, z: 7.0 µm × 2.5 µm × 1.0 µm; dwell time = 0.2 µs and overlap = -50 %). After the tungsten deposition, the spider silk was cut using the FIB so that a small piece of silk was attached to the AFM tip at its free end. Then the micromanipulator was moved close to one of the metal blocks and the free end of the fibre was carefully placed on the metal block for taping (Figure 2.8). After the fixing of the free end on the metal block by tungsten deposition, the spider silk fibre specimen was ready for testing.
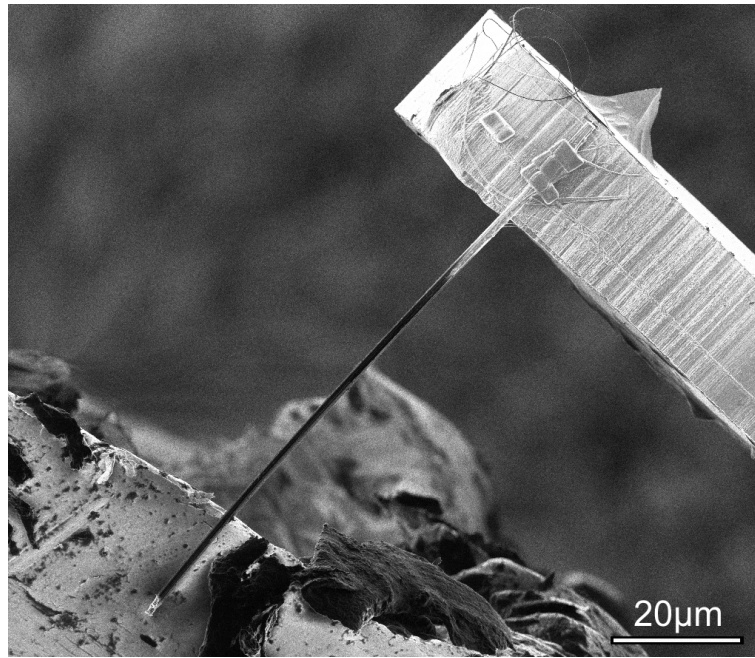
Figure 2.8: Spider silk affixed to the AFM tip with tungsten tapes and in contact
with a metal block at its free end (FIB micrograph).

Both tensile sample preparation techniques require an optimal alignment of the metal block, the sample and the AFM tip. The sample has to be affixed perpendicular to the AFM tip. The fixation of the sample on the metal block should happen in a way that the tungsten fixation tapes are also oriented perpendicular to the sample. An angle between the pulling direction of the manipulator and seta causes an error in the force measurement. However, knowing the angle between the specimen and the moving direction of the AFM tip, forces can be corrected accordingly.

2.4 *In situ* beam bending

The first mechanical tests performed with the new testing device were beam bending experiments. The samples were produced as described in Chapter 2.3. The beam bending experiments were performed inside an SEM (Leo 1530 VP). The setup for the beam bending experiments consists of the testing unit (micromanipulator with the attached AFM tip, Figure 2.1), and a personal computer, which controls the movement of the micromanipulator and monitors the force during the tests via the BIOPAC system (BIOPAC). The beam bending test method ran almost fully automated, controlled by two computers: the personal computer which controls the micromanipulator and the system computer of the SEM.

Testing procedure

The testing device was fixed to the stage of the SEM with a custom made holder so that both could be moved together (Figure 2.2). The specimen was held on a mini-vice and mounted on the sample tray. The AFM tip was moved close to the specimen before the sample chamber was evacuated. For testing, the AFM tip was moved to the testing position at the specimen. The drive of the micromanipulator was changed into the smallest gear, so that the micromanipulator could move through almost the whole range of its displacement of the smallest gear (from step -2048 to +2048 which corresponds to 61.4 μm for a fully extended and 32.8 μm for a fully retracted longitudinal axis of the micromanipulator). After bringing the AFM tip into contact with the sample, the BIOPAC hardware reads out continuously the force measured with the AFM tip and plotted it against time (500 samples per second). Figure 2.9 shows the AFM tip close to the cantilever, ready for testing.
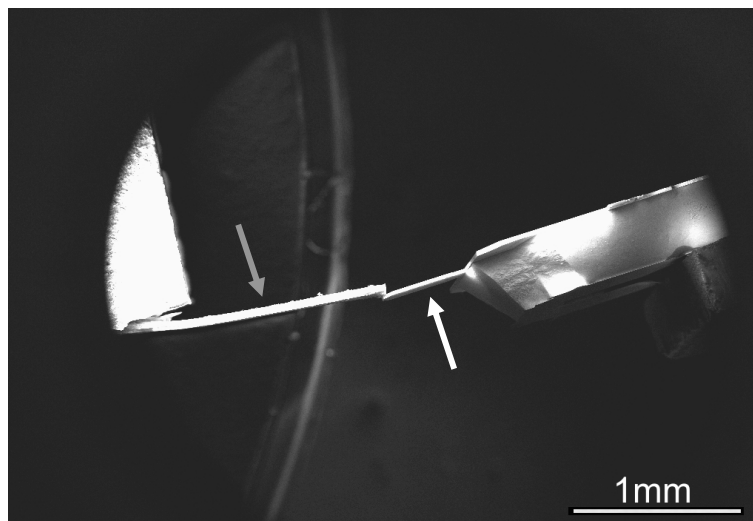

Figure 2.9: AFM tip close to the cantilever, ready for testing. The white arrow indicates the piezoresistive AFM tip, the grey the sample cantilever (SEM micrograph).

The bending test was controlled by AutoIt v.3.0.102 (AutoIt, 2004) macros. The SEM took a micrograph and stored it in a folder. At the same time the testing-time, the mean force of 705 samples and its standard deviation, as well as the minimum and the maximum forces were recorded with the BIOPAC system and copied into an Excel file. The filename of each micrograph taken was also stored in Excel. For the next measurement at a higher load the manipulator was moved a given number of fine steps (ranging from 1-128 steps, which corresponds to a distance of 8 nm to 1.92 μm) and the procedure performed as described above.

The loading of the sample continued until the maximum number of steps was reached and the sample was unloaded with the same number of measurements. Finally, a picture was taken and the force measured as described above. The macro for the testing procedure in bending is described in detail in Appendix 6.4.

In the elastic regime, the Young's modulus of a cantilever sample can be determined from the force deflection curves according to the following equation (Gere and Timoshenko, 1984):

$$\delta = \frac{F \cdot l^3}{3 \cdot E \cdot I_M}$$
[2.1]

Where δ is the deflection, F the applied load, l the length of the cantilever, E the Young's modulus and I_M the second moment of area. The second moment for a rectangular cross-section is:

$$I_M = \frac{w \cdot h^3}{12}$$
[2.2]

where w is the width and h the height of the cantilever. The second moment of area for a cylindrical beam of radius r is:

$$I_M = \frac{\pi \cdot r^4}{4}$$
[2.3]

With Equations [2.1] and [2.2], the Young's modulus E of a rectangular cantilever is:

$$E = 4 \cdot \frac{F}{\delta} \cdot \frac{l^3}{w \cdot h^3}$$
[2.4]

Using Equations [2.1] and [2.3], the Young's modulus E of a cylindrical cantilever is obtained as:

$$E = \frac{4}{3} \cdot \frac{F}{\delta} \cdot \frac{l^3}{\pi \cdot r^4}$$
[2.5]

The dimensions l, w, h and r were measured in an electron microscope and F/δ is the slope of the load-displacement curve in the elastic region of the unloading curve. The error calculation for the measurements is given in Appendix 6.3.

2.5 *In situ* tensile testing

The FIB was used as an *in situ* laboratory for the tensile tests. The whole test of a sample, first the sample preparation (Chapter 2.3), then the actual test, and finally the measurement of the cross-sectional area, was performed inside the FIB (fei 200 xP) without having to remove the sample from the chamber. Figure 2.10 shows a schematic of the tensile testing method.
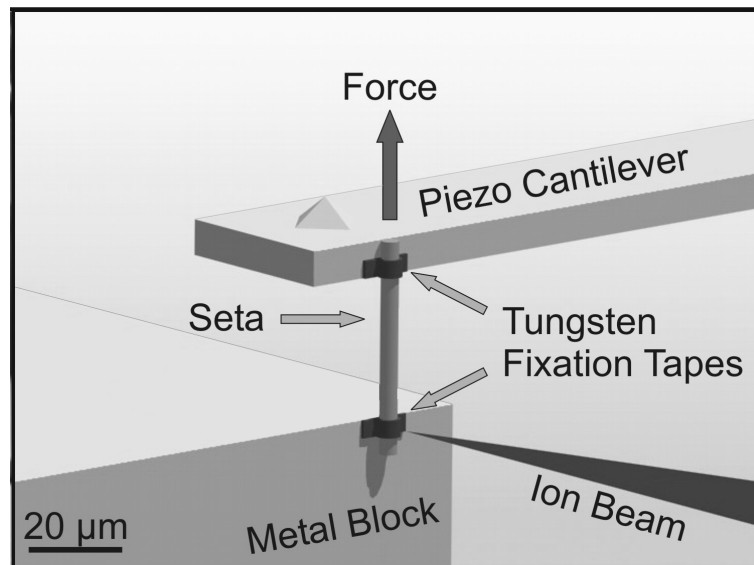

Figure 2.10: Schematic of the tensile testing method. The specimen is fixed with tungsten tapes between the metal block and the AFM tip.

In contrast to the beam bending experiments, the tensile testing was not fully automated, due to the lack of computer communication between the FIB computer and that which operates the micromanipulator. The tensile tests were performed *semi* automated via another AutoIt v.3.0.102 macro: The FIB user took a micrograph of the specimen, stored the micrograph in a file and started an AutiIt macro, which recorded the testing-time, the mean force value and its standard deviation, as well as the minimum and the maximum force values with a BIOPAC system. All data were stored with the filename of the micrograph in Excel. For the next measurement, the AFM tip was moved by a number of steps (1 to 128 steps). Then the user took another micrograph and the procedure was repeated. The test was continued until the sample broke. At the end of each test, the cross-sectional area of the sample was measured, using the method described in Chapter 2.7. The macro used for tensile testing and the error calculation for the tensile test results are described in Appendices 6.3 and 6.4.

2.6 Force and strain analysis

While direct force measurements were possible with the AFM tip, strain could not be measured with sufficient accuracy with this device due to a hysteresis in the piezoelectric motors of the micromanipulator. The solution to this problem was found in direct, and thus more accurate, measurements of sample strain by image analysis of micrographs taken during the test.

In the beam bending experiments, which were performed *in situ* in the SEM Leo 1530 VP, an SEM micrograph was taken after each stepwise increase in load applied by the AFM tip (Chapter 2.4). Using the software AutoIt v.3.0.102, Coral Draw 10 and Excel, a macro was written for strain analysis. Sequentially, one micrograph after another was opened after the test and a box drawn over a feature common to all micrographs. The positions of the box expressed in x-y-coordinates were stored automatically in Excel. Using the length of the micrometer bar in the micrograph expressed in x-y-coordinates, the displacement could be converted from x-y-coordinates into real displacements (see Appendix 6.4 for details of the macro). Combining measurements of the displacement with the respective force measurements, a force displacement plot was generated. While this method of displacement measurement worked well for beam bending experiments, it was not sufficiently accurate for tensile tests.

For the tensile tests, which were performed *in situ* in the FIB (fei 200 xP), another method was used, also based on the software AutoIt v.3.0.102. It allows direct strain measurements using grey values and their shift in pixels in FIB micrographs along a straight line drawn along the specimens. First, the grey values along a line were extracted using ImageJ (Rasband, 2004). The grey values were automatically stored first in an Excel file and then, again automatically, copied into an Origin 7 file. In Origin 7 the grey values were plotted and a peak at each end of the specimen was selected, fitted with a Gaussian fit and the position of its maximum stored in Excel. The change in distance between the two peaks was calculated for each of the micrographs, as shown in Figure 2.11. From these the strain could be calculated with the resolution of half a pixel divided by the pixel-length of the sample, which for an image size of 1024×881 pixel corresponds to strain resolution of 4×10^{-4} (0.04 %) at best, when the sample is in the diagonal of the micrograph, using the maximum length, a length of 1350 pixel in the micrograph (see Appendix 6.3 for calculation of the strain resolution and Appendix 6.4 for a detailed description of the macro).
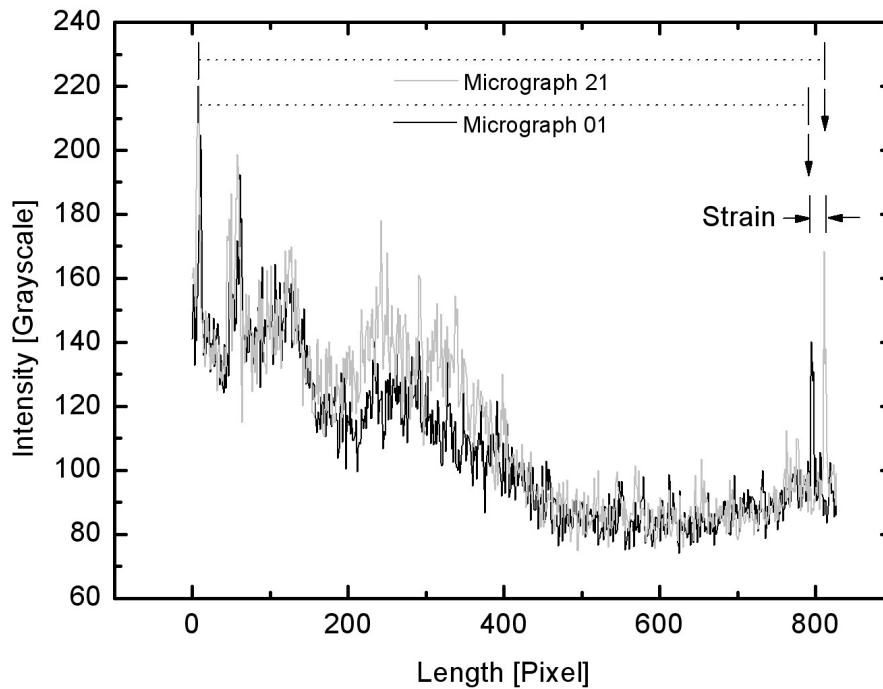
Figure 2.11: Gray values along the seta. By measuring the displacement of one peak at each end of the seta it is possible to calculate the strain during the tensile test.

2.7 Measurement of the cross-sectional area

To convert forces into stress, the cross-sectional area of the sample was determined from micrographs of FIB prepared cross-sections, illustrated in the following taking a seta of the beetle *Gastrophysa viridula* as an example. Starting at the fractured end, cross-sections were milled at discrete positions along the sample length using the fine milling tool of the FIB. To measure the cross-sectional area, the stage of the FIB was tilted by 45° and micrographs were taken. Using the software Coral draw 10, the cross-sectional area was outlined and the image was converted into a real black and white picture. Black was the area of the cross-section and white was the rest of the image, including pores within the sample (Figure 2.12). This was always done twice for each picture, marking a minimum and maximum area, because the edges of the cross-sections frequently appeared rounded. Using Coral Photo-Paint 10, a histogram was plotted for the "grey values" of the pictures. The histogram gives a mean value for the "greyscale". Dividing this value by a factor of 255, the value for "white, the percentage of "white" in the picture, and thus the percentage of "black", or sample area, can be calculated and then converted from pixels to μms. Finally, the cross-sectional area at 0° can be calculated from that at 45° tilt. Figure 2.12 shows the micrographs of the cross-sections, the outlined cross-sections and the mean value of each cross-sectional area. The advantage of this method is that the real cross-sectional area can be measured and used in the

calculation of stresses. This is of particular advantage for complex, porous or hollow structures.
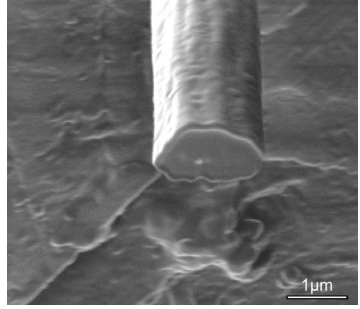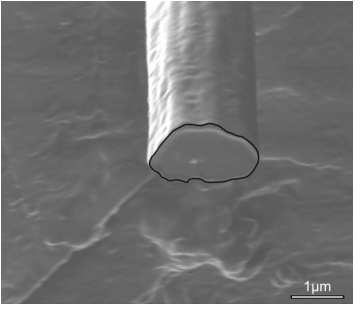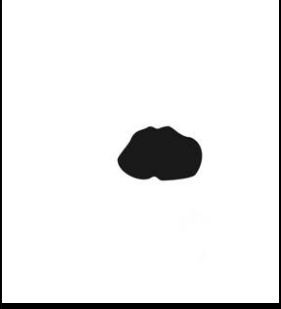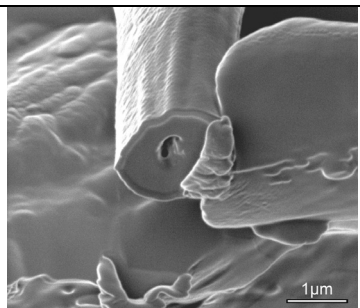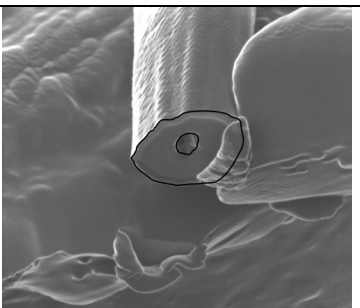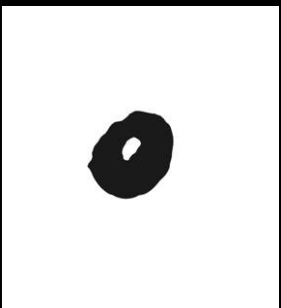
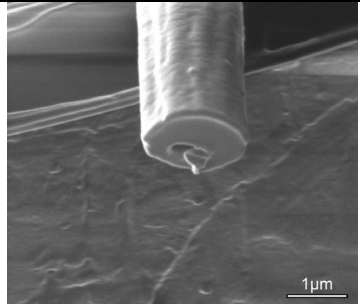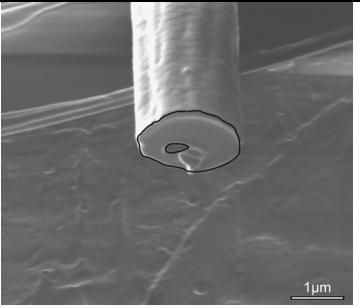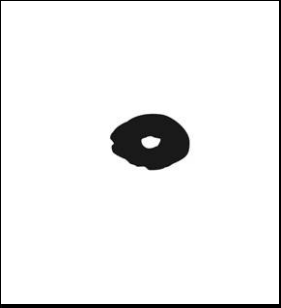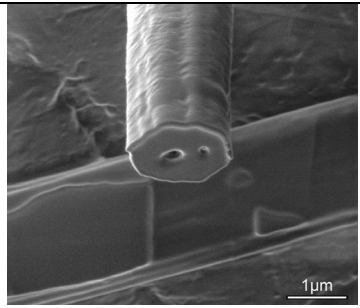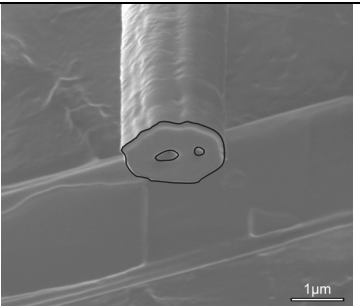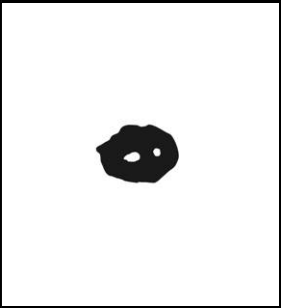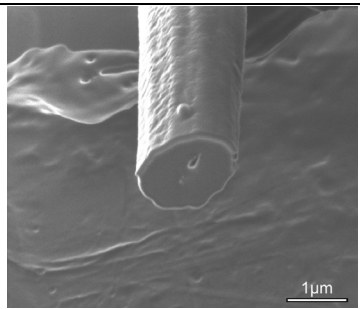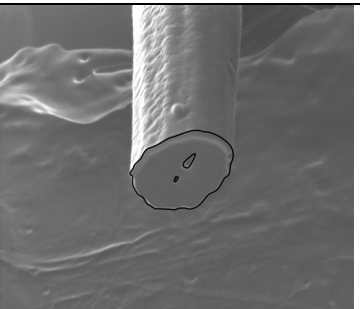| Original	Cross-section	Cross-section in black and white	Calculated area [µm²]
			1.76
			1.65
			1.71
			2.05
			2.41

Figure 2.12: Measurement of the cross-sectional area of a seta of *Gastrophysa viridula* (FIB micrographs; beam current: cutting = 150 pA, cleaning = 11 pA).

2.8 Discussion

The FIB was used as an *in situ* laboratory for sample preparation, fixation, mechanical testing and the measurement of th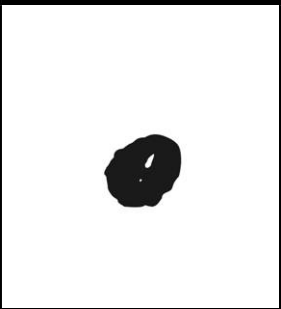e sample dimensions before and after the test. The positioning accuracy of the micromanipulator allows the mounting of small samples with high accuracy. Samples with a diameter of ~1 μm and several tens of μms in length can easily be handled. The use of the FIB system, especially its milling and GAD processes, allow to micromachine and to affix the samples to the testing device, which is otherwise not trivial. After tests in bending and in tension cross-sections of the tested samples were prepared to measure the cross-sectional area, which is particularly important in the case of hollow or porous samples. Conventional techniques usually do not provide the possibility to determine the sample cross-sectional area. The strengths and weaknesses of the novel testing method are discussed in detail, below.

Advantages of the *in situ* method

The *in situ* testing method presented here is well suited for mechanical testing of samples in the μm-range, which is an important size range in biological structures as illustrated in Chapter 1.4. For the force measurements, piezoresistive AFM tips with a force resolution of 15-20 μN and a maximum force of 1300 μN were used. Strains could be measured with a maximum resolution of 0.04 %. Figure 2.13 shows the force ranges (force resolution to maximum force) plotted versus the displacement ranges (displacement resolution to maximum displacement) for small scale *in situ* mechanical testing methods described in the literature.

It illustrates that the *in situ* testing method developed during this thesis is unique, no other *in situ* testing method spans a comparable force and displacement range.

One of the major advantages of this new testing method is its versatility: The use of the micromanipulator as a force measuring device allows to perform bending and tensile tests inside an SEM or FIB system. It is also possible to perform mechanical tests under a light microscope, because the present testing method is not restricted to be used in only one fixed setup or environment: the force can be directly measured by the AFM tip, and the strains can be measured on digital images of the sample taken during the tests.
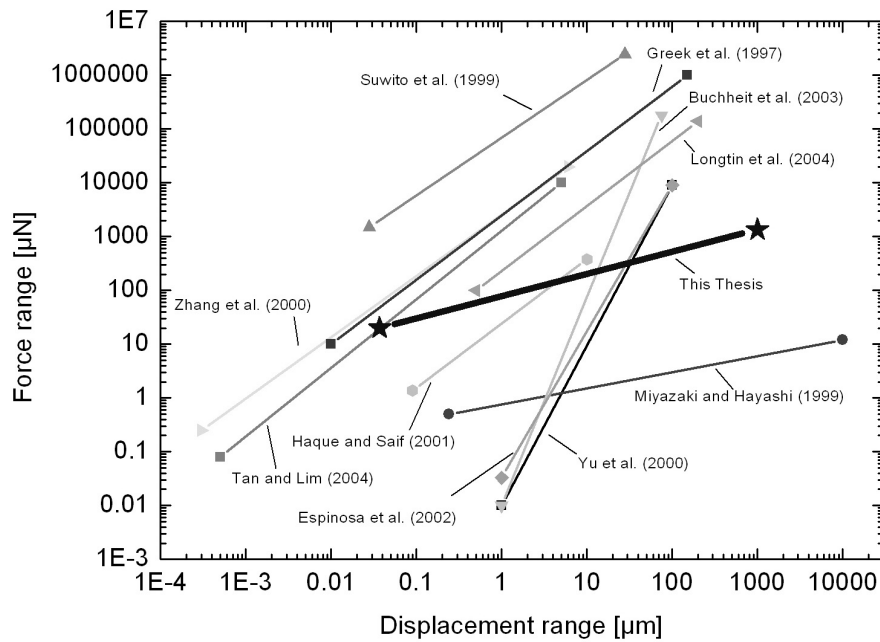
Figure 2.13: Force and displacement ranges of the *in situ* small scale mechanical testing methods found in the literature compared with the testing method presented here.

The testing method was initially designed for the testing of biological samples in the μm-range. However, it is not restricted for their testing. Due to the sample preparation techniques and the mounting of the samples, already a variety of technical samples could be tested successfully, as described in Chapter 3. In contrast, most mechanical testing methods described in the literature are much more specialised and frequently for one specific application only. The methods of Greek *et al.* (1996), Buchheit *et al.* (2003), Haque and Saif (2002) and Suwito and Dunn (1999) also need custom made samples for testing and are not suited for the testing of biological samples.

Sample preparation using the FIB has some advantages. Samples can be fabricated without artefacts due to mechanical cutting or thinning, which occur if the samples are cut using a razorblade or a diamond saw. With these methods the possibility of the insertion of micro-cracks into the material is always present, and plastic deformation can occur at the cutting edge. Using the FIB, the sample can be prepared with high accuracy and site specifically. This is of particular interest for the investigation of composite materials: a sample of each of its components can be micromachined and their mechanical properties can be measured independently.

Also the sample fixation with tungsten tapes deposited in the FIB has an advantage: tight sample clamping can cause mechanical damage to brittle and soft materials. Cracks or stress

concentrations can be introduced leading to a reduced tensile strength of the overall sample. In some mechanical tests (Miyazaki and Hayashi, 1999; Suwito *et al.*, 1999) the strain is measured from the relative displacement of the sample grips. This can cause some artefacts: if the sample is not clamped tightly enough, the sample can slip out of the sample holder and the measured strain is bigger than the real strain of the sample. The tungsten tapes were not only shown to be strong enough to fix the sample, they also allowed strain measurement on the sample so that even a slight slip of the fixation tapes did not affect the accuracy of the strain measurement.

The force is applied to the sample by displacing the AFM tip in a stepwise manner with the micromanipulator. The step size can be varied from one step (< 6 nm) in the smallest gear, to several steps (several μm) in higher gears. By changing the step size of the micromanipulator, the strain rate can be varied. This is of interest for the testing of viscoelastic specimens, where the mechanical properties of the material are highly strain-rate dependent. Since the time is always recorded during the test and stored together with the micrograph identification and the force value, the strain rate can be calculated for each test. For the tensile test on the single seta in Chapter 3.3.1 a strain rate of 2 nm/s (= 0.006 %/s) was used, for example.

If the sample is not perfectly aligned (not perpendicular to the AFM tip), the real force along the tensile sample will be smaller than the applied force. The force will split up into two components, a longitudinal force (along the sample) and a second component normal to it. Here the *in situ* testing is an advantage, because the angle between the AFM tip and the sample can be measured from the micrographs taken during the mechanical tests and be taken into account in the calculations.

The strain can be measured with high resolution. In the case of the tensile tests, the strain resolution depends on the imaging resolution of the FIB and the pixel-resolution of the micrographs. The spatial resolution of the FIB is about 6 nm, it provides high resolution for the measurement of deflections in the nm-range, which was found to be advantageous for the samples tested. The limiting factor was the pixel resolution of the micrographs, since the strain was measured by fitting the intensity of the grey values of each pixel along a line on the sample. Using the highest resolution of 1024×881 pixels in the FIB (fei 200 xP), a strain resolution of ± 0.04 % can be achieved.

Another benefit of the strain measurement from the micrographs is that it offers the possibility of measuring strain gradients by monitoring different peaks in the grey values along the sample length. If the specimen surface is so smooth that peaks due to surface roughness do not exist, tungsten tapes can be deposited as markers at discrete distances. It should even be possible to measure the transverse strain of the sample, and all strain measurements can be performed on the same sample and in a single test.

The *in situ* observation of the sample during the test has another advantage. The formation and distribution of cracks can be monitored. The force is also monitored so that the force at the beginning of the cracks and the force necessary for the growth of these cracks are known.

Disadvantages of the present testing method

A possible problem with this dry-mount method, however, is the presence of a vacuum during sample preparation and testing. The mechanical properties of biological materials can change considerably upon hydration. The measured values may thus not fully represent the *in vivo* state. However, the testing of dry samples is also advantageous: it is a reference state that is quickly and reproducibly achieved in vacuum. By contrast, the frequently reported 'natural' or 'wet' state is less well defined.

Another disadvantage is that the Ga^+-ion beam interacts with the sample and introduces damage into the biological materials. As described above in Chapter 1.6, it affects the mechanical properties of polymers. However, since the influence of the ion beam is limited by the stopping range of the ions in the material and depends on the thermal conductivity of the material, it could be neglected for samples tested here, since they were significantly larger than the affected volume, as shown in Chapter 1.6.

Beam bending versus tensile testing

The mechanical tests described in the literature, bending tests, tensile tests and compression tests, are all possible with the *in situ* device, each has advantages and disadvantages. They are described in the following chapter.

Affected volume

One major difference between tensile testing and beam bending is the affected volume, since the stress distribution in a beam is not uniform, while in a tensile specimen it is. In beam bending, it increases linearly from the neutral axis towards the surfaces and is highest at the top (tension) and bottom (compression) side of the fixed end of the cantilever. By contrast, the stress in a tensile specimen is uniform over the cross-sectional area. Deviations from this are due to geometrical effects or the composite structure of the sample. In tension, dog bone shaped samples are preferred since this ensures failure in the middle of the sample rather than at its ends, which are affected by the gripping of the sample.

Geometry effects

For beam bending samples, the knowledge of the exact geometry is necessary for the calculation of the Young's modulus (Equations [2.4] and [2.5]). If the geometry is very complex and if the material tested is a composite of unknown structure, it is often easier to cut a micro-beam with a simple geometry out of the material. The tensile testing method has an advantage: the cross-sectional area can be measured much more easily than the second moment of area, particularly for composites. Several biological samples could be tested in their natural state, with very complex geometries, as described in Chapter 3.

2.9 Conclusions

Sample preparation using the FIB system is straightforward: samples can be prepared site specifically and in a shape and size ideal for beam bending as well as for tensile tests. For both, the samples stiffness was estimated before testing and the sample geometry adjusted accordingly. The ability to test small scale samples makes the investigation of highly hierarchically structured samples possible, in which the size of the sample limits the level of hierarchy which can be explored.

The tungsten tapes used for mounting tensile samples provide a stable fixation and eliminate gripping effects due to clamping. This makes the newly developed *in situ* testing method well suited for mechanical testing of samples in the μm-size range, which are otherwise difficult to handle. The force resolution of 15 to 20 μN, a maximum force of 1300 μN and a strain resolution of about 0.04 to 0.06 % was found to be ideal for the testing of biological samples and their structures, which often are only a few μm in size. The testing method described in this thesis thus fills a gap in the existing *in situ* mechanical testing devices used for small scale samples (Table 2.1, Figure 2.13).

Another strength of the new method is that it allows testing in bending and tension, not only in an SEM or FIB system, but also under an optical microscope, because forces are measured directly via the AFM tip and the strains can be determined from micrographs taken during the tests. Measuring strains by image analysis has some important advantages. The strain can be measured with high resolution and the mechanical test can be observed *in situ*. This means that the behaviour of the sample, especially the nucleation and propagation of cracks can be investigated as well as material property gradients in the material.

2.10 References

AutoIT, Version v3.0.102 (2004) Jonathan Bennett & AutoIt Team, (avajable from www.autoitscript.com)

BIOPAC Systems, Inc. (Model No. MP100A-CE), 42 Aero Camino, Goleta, CA 93117, USA

Buchheit T.E., Glass S.J., Sullivan J.R., Mani S.S., Lavan D.A., Friedmann T.A. and Janek R. (2003) "Micromechanical testing of MEMS materials" *Journal of Materials Science* **38**, 4081-4086

Ding J.D., Meng Y.G. and Wen S.Z. (2001) "Specimen size effect on mechanical properties of polysilicon microcantilever beams measured by deflection using a nanoindenter" *Materials Science and Engineering* B **83**, 42-47

Espinosa H.D., Prorok B.C. and Fischer M. (2003) "A methology for determining mechanical properties of freestanding thin films and MEMS materials" *Journal of the Mechanics and Physics of Solids* **51**, 47-67

Florando J., Fujimoto H., Ma Q., Kraft O., Schwaiger R. and Nix W.D. (1999) "Measurement of thin film mechanical properties by micro beam bending" *Material Research Society Symposium Proceedings* **563**, 231-236

Florando J. and Nix W.D. (2001) "Study of the yielding and strain hardening behaviour of a copper thin film on a silicon substrate using microbeam bending" *Material Research Society Symposium Proceedings* **673,** P1.9.1-P1.9.6.

Gere J.M. and Timoschenko S.P. (1984), *Mechanics of Materials*, 2nd edition, PWS-Kent Publishing Company, Boston, USA

Gorb S.N. (2000) *Attachment Devices of Insect Cuticle* Kluwer Academic Publishers, Dordrecht

Greek S., Ericson F., Johansson S. and Schweitz J.-Å. (1996) "In situ tensile strength measurement and Weibull analysis of thick film and thin film micromachined polysilicome structures" *Thin Solid Films* **292**, 247-254

Haque M.A. and Saif M.T.A. (2001) "Microscale materials testing using MEMS actuators" *Journal of Microelectromechanical Systems* **10(1)**, 146-152

Haque M.A. and Saif M.T.A. (2002) "Application of MEMS force sensors for in situ mechanical characterisation of nano-scale thin films in SEM and TEM" *Sensors and Actuators* **A 97-98**, 239-245

Hoshi K., Ejire S., Probst W., Seybold V., Kamino T., Yaguchi T., Yamahira N. and Ozawa H. (2001) "Observation of human dentine by focussed ion beam and energy-filtering transmission electron microscopy" *Journal of Microscopy* **201**, 44-49

Huang H. and Spaepen F. (2000) " Tensile testing of free-standing Cu, Ag and Al thin films and Ag/Cu multilayers" *Acta Materialia* **48**, 3261-3269

Keil T. A. (1998) *The structure of Integumental Mechanorezeptors Microscopic Anatomy of Invertebrates* Volume 11B Insecta Wiley-Liss, Inc., USA, pp. 385-404

Kleindiek Nanotechnik GmbH, Aspenhaustrasse 25, D-72770 Reutlingen, Germany.

Longtin R., Fauteux C., Pegna J. and Boman M. (2004) "Micromechanical testing of carbon fibers deposited by low-pressure laser-assisted chemical vapour deposition" *Carbon* **42**, 2905-2913

Lui D., Weiner S. and Wagner H.D. (1999) "Anisotropic mechanical properties of lamellar bone using miniature cantilever bending specimens" *Journal of Biomechanics* **32**, 647-654

Miyazaki H. and Hayashi K. (1999) "Tensile tests of collagen fibers obtained from the rabbit patellar tendon" *Biomedical Microdevices* **2:2**, 151-157

Nascatec GmbH, Ludwig-Erhard-Straße 10, D-34131 Kassel, Germany.

Rasband, W. ImageJ (Version 1.32j), National Institutes of Health, USA, (available from http://rsb.info.nih.gov/ij/, 2004).

Serre C., Gorostiza P., Pérez-Rodríguez A., Sanz F. and Morante J.R. (1998) "Measurement of micromechanical properties of polysilicone microstructures with an atomic force microscope" *Sensors and Acuators* **A 67**, 215-219

Stokes D.J. and Donald A.M. (2000) "*In situ* mechanical testing of dry and hydrated breadcrumb in an environmental scanning electron microscope (ESEM)" *Journal of Materials Science* **35**, 599-607

Suwito W., Dunn M.L., Cunningham S.J. and Read D.T. (1999) "Elastic moduli, strength, and fracture initiation at sharp notches in etched single crystal silicon microstructures" *Journal of Applied Physics* **85(7)**, 3519-3534

Tan E.P.S. and Lim C.T. (2004) "Novel approach to tensile testing of micro- and nanoscalefibers" *Revier of Scientific Instruments* **75(8)**, 2581-2585

Uchic M.D., Dimiduk D.M., Florando J.N. and Nix W.D. (2004) "Sample dimensions influence strength and crystal plasticity" *Science* **305**, 986-989

Yu M-F., Lourie O., Dyer M.J., Moloni K., Kelly T.F. and Ruoff R.S. (2000) "Strength and breaking mechanism of multiwalled crabon nanotubes under tensile loading" *Science* **287**, 637-640

Zhang T.-Y., Su Y.-J., Qian C.-F., Zhao M.-H. and Chen L.-Q. (2000) "Microbridge testing of silicon nitride thin films deposited on silicon wafers" *Acta Materialia* **48**, 2843-2857